ELSEVIER

Chemical Engineering Journal 129 (2007) 31–40

Chemical Engineering Journal

www.elsevier.com/locate/cej

Catalyst layer in PEMFC electrodes—Fabrication, characterisation and analysis

N. Rajalakshmi *, K.S. Dhathathreyan

Centre for Fuel Cell Technology, International Advanced Research Centre for Powder Metallurgy and New Materials (ARCI), 120, Mambakkam Main Road, Medavakkam, Chennai 601302, India

Received 29 April 2006; received in revised form 24 October 2006; accepted 29 October 2006

Abstract

A new and simple process has been developed for the fabrication of catalyst layer of the PEMFC electrodes, scalable to large area electrodes in order to reduce the interfacial contact between the catalyst layer and the electrolytes. The catalyst layers of the PEMFC electrodes prepared by this process have been structurally characterized by EDAX and SEM studies. The fuel cell experiments carried out on the laminated electrode membrane assembly (EMA) were analysed, in order to get the dependence of the performance of the fuel cell electrode on proton network, electronic network and interface between the electrolyte and the electrocatalysts. The interfacial resistance has been evaluated for EMAs made by conventional method and the new process and compared. The catalyst layer prepared by this process showed higher platinum utilization in the electrodes and also amenable for scaling up.

Keywords: Fuel cells; PEMFC; Electrocatalyst; Decal; Screen printing

1. Introduction

Research activities in proton exchange membrane fuel cells (PEMFC) have gained much momentum during the past decade [1]. Understanding the relationship between structure, properties, processing and performance is an essential prerequisite in the search for cost effective materials in PEMFC. The important challenges in PEMFC research arise in their catalyst layers because they are complex and heterogeneous. The catalyst and catalyst layers are required to be designed so as to generate high rates of desired reactions and minimize the amount of catalyst required for reaching the required levels of power output. In addressing these issues, a few requirements need to be considered: (1) large interface between the polymer electrolyte and catalyst, (2) efficient transport of protons generated at the anode and consumed at the cathode at the reaction spots, (3) easy transport of reactant or product gases and removal of condensed water, and (4) continuous electronic current passage between the reaction spots and the massive current collector. The overall catalyst layer performance depends on all these critical factors and is therefore essential to identify the composite structures and operation conditions which provide the best balance between them. The improvement of catalytic activity is a task of material chemistry and in view of the competing requirements, the optimum structure is a result of trade off between all the four requirements. Most of the known fabrication procedures like spraying, painting, rolling, screen printing, etc., reveal hardly any degree of precision and there is not much control over the composite structures of fabricated membrane electrode assemblies [2–5]. Screen printing is also one of the most popular methods used for the fabrication of catalytic layer either in the membrane or in the electrode of the PEMFC [6]. In the direct printing or screen printing process, the catalyst slurry was applied to the membrane in Na^+ form or TBA (tetra butyl ammonium) form to stabilize the catalytic layer enhancing the physical strength of the membrane. However, there are no reports on the potential impact of these methods on the precision of resulting catalyst loading, effect of changes in material parameters such as ink composition, type of coating, substrate, etc. A series of parameters affecting the catalytic layer microstructure in polymer exchange fuel cell electrodes have been studied by Fernandez et al. [7] in which they have shown that the deposition of the catalytic layer in the gas diffusion support depend not only on the ink deposition method but also on the charac-

* Corresponding author.
E-mail address: lakshmiraja2003@yahoo.com (N. Rajalakshmi).

1385-8947/$ – see front matter © 2006 Elsevier B.V. All rights reserved.
doi:10.1016/j.cej.2006.10.035

teristics of the solvent used to disperse both the catalyst and the Nafion ionomer. The solvent viscosity and its dielectric constant are two important factors to control for the catalytic ink preparation. In particular, the solvent dielectric constant is shown to be directly related to the electrode performance in single cell tests. The differences in fuel cell performance resulting from different preparation procedures has been studied by Frey and Linardi [8] and identified an optimized fabrication concept with regard to maximal performance, considering the previous optimized procedure. A novel method based on the electrospray technique has been developed by Ben'ýtez et al. [9] and characterized by different techniques, which showed both morphological and structural improvements that contribute to a better catalyst utilization compared to conventional methods. These facts were corroborated after manufacturing several electrode membrane assemblies (EMAs) with electrodes prepared by three different methods. EMAs obtained by means of the electrospray technique exhibited three times higher power density than those prepared by the impregnation method ones and eight times higher than EMAs made with electrodes prepared by the spray technique with platinum loadings of 0.5 mg cm^{-2}. Moreover, the power density obtained was twice better than a commercial E-TEK. However, the same group has studied the platinum utilization in electrodes prepared by impregnation, spray and electrospray methods and found that the impregnation method gives a higher platinum utilization than the other two methods and they have attributed the same for complete solvent removal in the case of impregnation due to long period leading to tortuous porous structure, while in the other two methods, immediate elimination of solvent leaves a low porous structure [10]. Xu et al. [11] recently reduced the Nafion content in the catalyst layer by incorporating sulphonic acid group in the carbon supported catalyst particles, thereby decreasing the resistivity and the performance was found to be higher than the unsulphonated counterpart. Kaz and Wagner [12] studied the triple phase boundary with different kind of catalysts and different amount of electrolyte in the electrode to explore the interrelationship between platinum and electrolyte content by the dry spray technique directly onto the membrane surface. They have found that the dry coated electrodes require a high amount of Nafion to the catalyst to increase the triple phase boundary. Santamaria et al. [13] studied the electrode performance by reduced the platinum loading to 50 μg/cm^2, which is about 10 times lower than the normal loading, in the catalyst layer by dc magnetic sputtering, They observed the same performance when oxygen is used as oxidant. However, the performance loss is high when air is used as oxidant and they have attributed the same to less porous catalyst layer by sputtering, than the standard catalyst layer. Giorgi et al. [14] described the preparation methods based on the electrochemical and sputter deposition of low-loading Pt nanoparticles on gas diffusion electrodes, as a tool for manufacturing proton-exchange membrane fuel cell (PEMFC) electrodes with improved performance and catalyst utilization versus commercial chemical deposited platinum. The porosity of the thin film decal method using Pt_3Cr catalyst has been studied by Xie et al. [15], where they found that the majority of pores for carbon powders and catalyst loaded carbon powders concentrate in a range from 24 to 84 nm with a small number of residual pores lying outside this range. The catalyst layer prepared from recast Nafion and carbon supported catalyst has different pore structure, determined by the type of catalyst used, the preparation method, and the total Nafion content. The catalyst layer has two distinctive pore categories which decreases with an increase of Nafion content which affects the performance of EMAs over the entire current range. The optimum performance was obtained with a Nafion content of 28 wt% for a Pt_3Cr catalyst layer made by the thin film decal process. The other method of EMA fabrication was by electrophoretic deposition (EPD) reported by Morikawa et al. [16], in which a suspension consisting of ethanol, carbon powders with Pt catalyst, and Nafion polymer was used in the EPD process to obtain a stable dispersed solution. The thickness of the prepared catalyst layer was controlled by EPD duration or concentration of suspension and the layer was similar to that prepared by a hot press method.

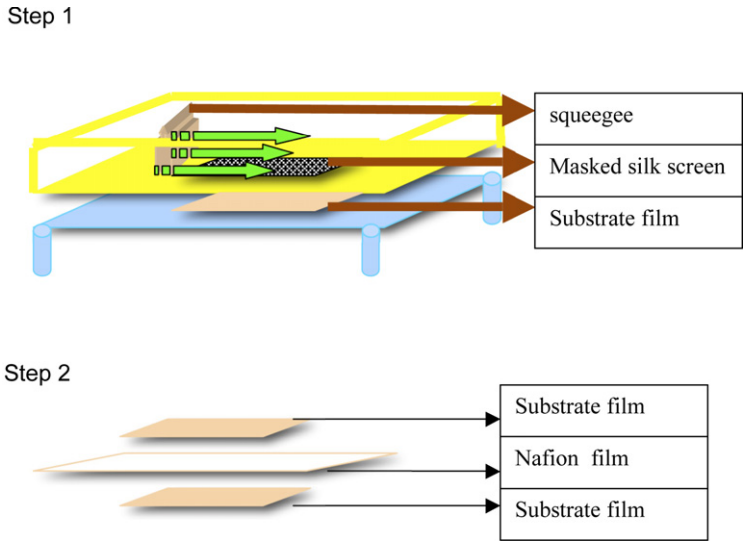

Fig. 1. Schematic of coating apparatus: (Step 1) at ambient conditions and (Step 2) at suitable pressure and temperature.

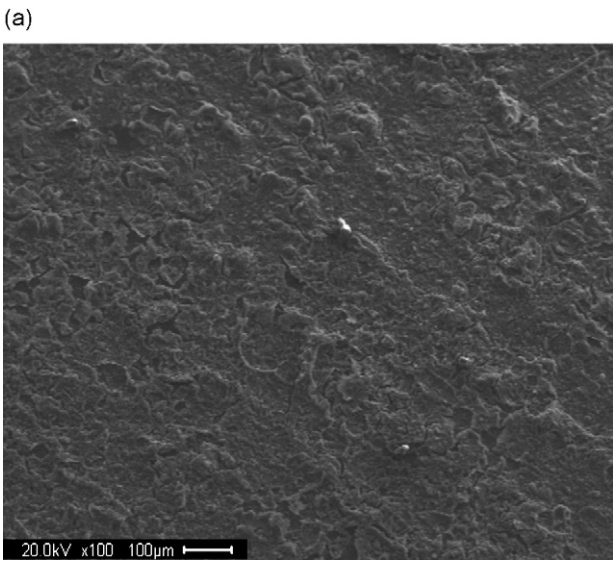

Fig. 2. SEM picture of catalyst layer. (a) Catalyst layer in decal film.

This method produced a uniform structure which in turn provided a 56% utilization of Pt catalyst. A method based on pulse electrodeposition technique was developed by Kim and Popov [17] for preparation of membrane electrode assemblies which ensures that most of the platinum to be in close contact with the membrane. Using this method it is possible to increase the Pt/C ratio up to 75 wt% near the surface of the electrode resulting in a 5 mm thick catalyst layer. The EMA prepared by pulse electrodeposition exhibits a current density of 0.33 A/cm^2 at 0.8 V with platinum loading of 0.25 mg of Pt/cm^2. The results indicate that pulse deposition may be an attractive technique to replace the conventional powder-type EMA preparation methods. Wu et al. [18] studied the effect of current distribution in the catalyst layer by a modified sub cell approach and showed that the conventional hydrophobic electrodes showed better performance under flooding conditions compared to hydrophilic electrodes. A composite catalyst layer was designed with 2/3 of the area from the inlet prepared hydrophilic and the remaining 1/3 area hydrophobic which showed a notable enhanced performance in the concentration polarization region. Saha et al. [19] fabricated EMAs using a thin preformed precursor sheet which was sandwiched between two gas-diffusion electrodes. An effective three phase boundary was established due to thermoplastic property of the precursor sheet, which showed an enhanced performance in single-cell tests at 75 °C, current density of 0.4 A/cm^2 at 0.5 V compared to conventional electrodes. Inaba et al. [20] studied the effect of agglomeration of Pt/C catalyst on hydrogen peroxide formation by rotating disk electrode and found that the formation of H_2O_2 was enhanced with a decrease in agglomeration of Pt/C.

In the present paper, we have developed a new process for the fabrication of catalyst layer by combining the screen printing and decal process in order to increase the interfacial contact between the membrane and the catalyst layer. The catalyst layer performance is analysed by electrochemical methods, current–voltage characteristics. Microscopic examination of the electrodes as well as interface and the elemental map analysis were carried out to get the structural relationship, adhesiveness of the catalyst with electrolyte and the distribution of catalysts.

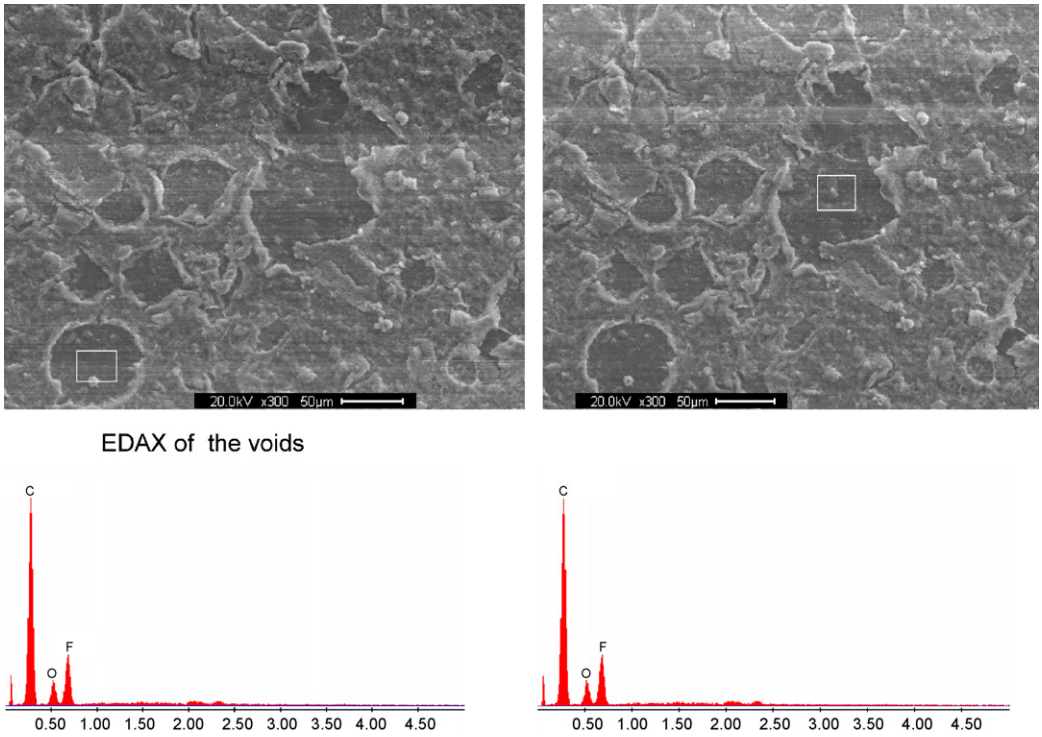

Fig. 3. SEM of catalyst layer on the kapton film and EDAX of the voids.

2. Experimental

2.1. Fabrication procedure

The coating apparatus consists of a silk screen of 100 mesh fixed to a wooden frame with proper tension to squeeze the ink through the screen to the polyimide blank. The substrate layer (polyimide blank) is fixed on the XY table with the help of adhesive tape. The silk screen mesh is completely masked with the help of a masking fluid, except the area to be screen printed. The squeegee, made of silicone rubber, is fixed in a wooden cavity, can be moved along both *X* and *Y* directions. A hot air dryer/IR lamp is fixed on the frame in order to dry the coating at every step for the removal of solvents.

Fuel cell catalyst ink was prepared by taking 20% Pt/C, (Arora Mathey, India), water and 5% Nafion solution from Dupont. The slurry was ultrasonicated till a good catalyst ink is formed. The coating procedure consists of positioning the substrate layer under the silk screen mesh, which is not masked, and squeegee on top of the mesh at one side. The schematic of coating facility is shown in Fig. 1. The appropriate amount of the ink is micropipetted near the squeegee and the slurry is spread across the mesh and then pushed through the mesh to the substrate layer by moving the squeegee quickly. The hot air heater is turned on to dry the catalyst layer coated on the substrate. The same procedure was repeated until the pipetted volume of catalyst ink is being transferred to the substrate layer. After coating, the substrate layer was dried for about 2 h. The area of the catalyst layer is 30 cm^2. Subsequently, Nafion 1135 membrane converted to Na^+ form was used to transfer the catalyst layer from the decal film, on both sides. This was done by using a hydraulic hot press. This procedure was repeated for both anode and cathode separately. After transferring the catalyst from the kapton film to Nafion membrane, the membrane was once again converted to acid form by boiling in concentrated sulphuric acid. Two gas diffusion electrodes of size 30 cm^2 made by a proprietary process were bonded to the catalyst-coated membrane. In a subsequent experiment the electrode size was increased from 30

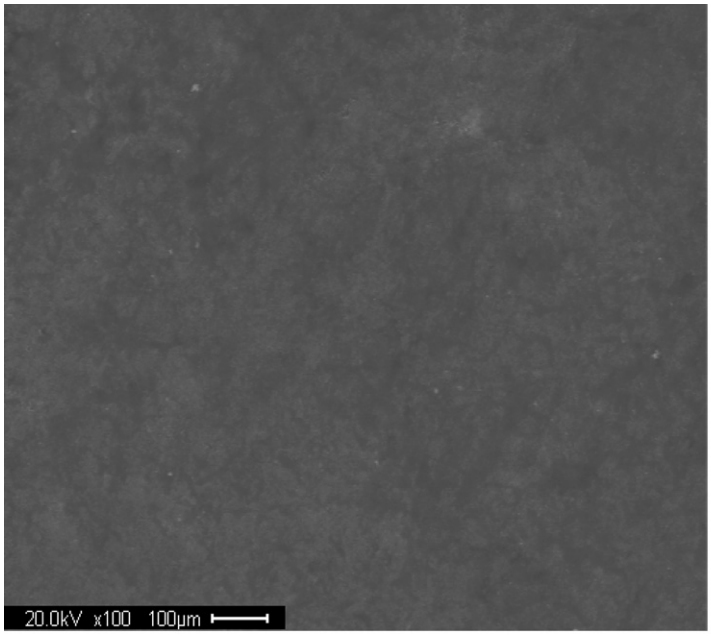

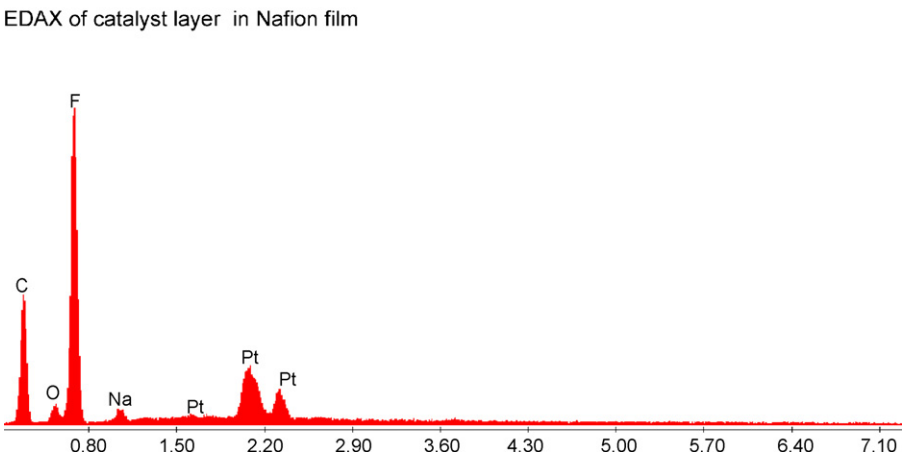

Fig. 4. Catalyst layer in the Nafion film after decal from the kapton film. EDAX of catalyst layer in Nafion film.

to 90 cm^2. This electrode is called decal electrode which combines both screen printing of catalyst layer and decaling the same to the electrolyte. Microstructural characterization was carried out by using a high-resolution scanning electron microscope (Hitachi). From the EDS examination, elemental map analysis was carried out for all the elements present in the catalyst layer. X-ray fluorescence analysis was carried out using a Philips XRF spectrometer for the laminated membrane electrode assembly by

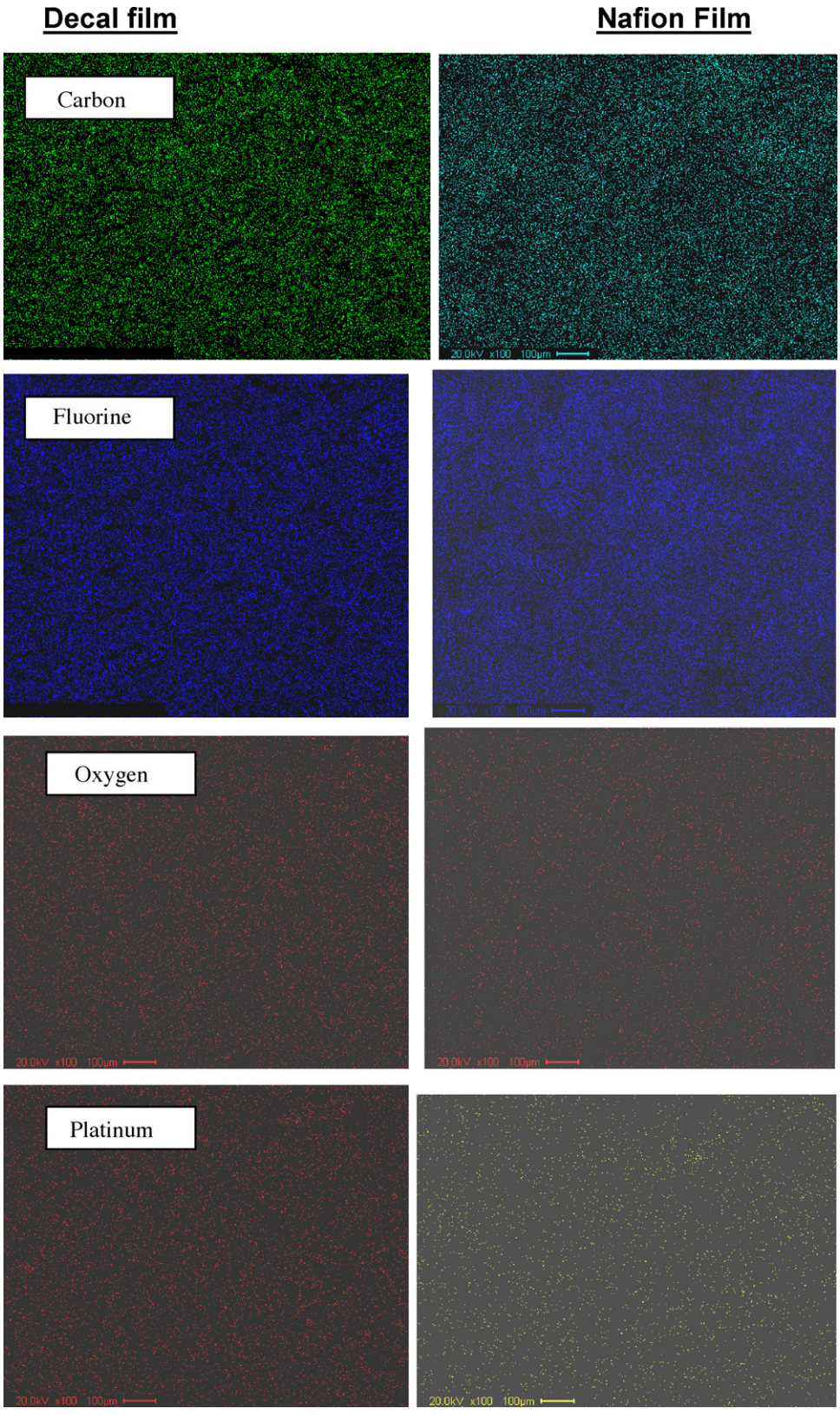

Fig. 5. Elemental map analysis of electrodes in decal film and Nafion film.

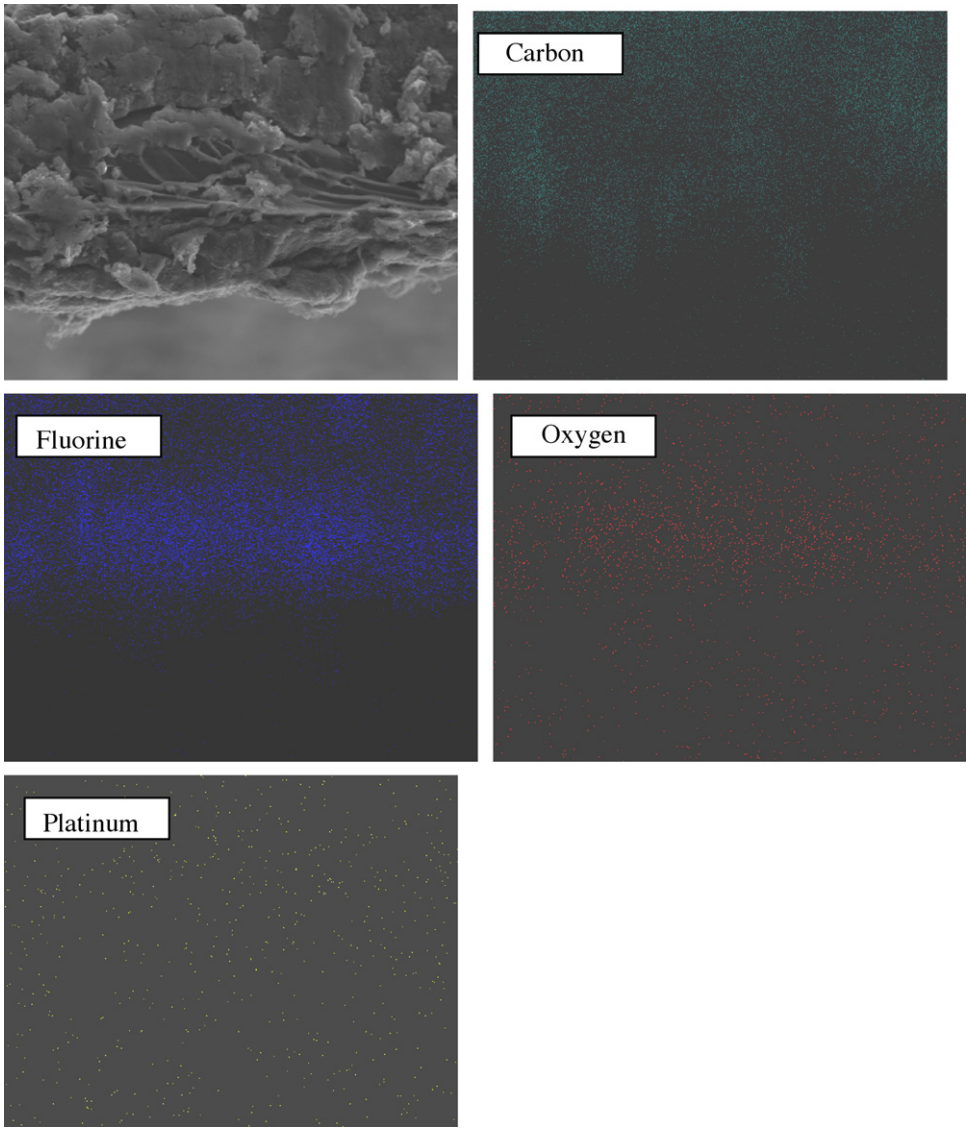

Fig. 6. SEM image of EMA (Pt decal) at the intersection.

inserting the same in the SS holder and tightening the same with the help of a plastic fixture.

2.2. Fuel cell testing

The EMAs thus made were inserted in the fuel cell hardware consisting of two graphite blocks with parallel flow field channels for the reactants, two copper current collector and an end plate assembly. Polarization measurements were carried out using a test bench facility fabricated in house, consists of gas supply chamber, humidity chamber, temperature control system and an electronic dc load box. The fuel and oxidant are H_2 and air in

Table 1
XRF elemental analysis of MEA

Element	Anode (wt%)	Cathode (wt%)
F	11.708	8.725
Mg	0.038	0.029
Si	0.58	0.211
Cl	0.199	0.074
Na	0.144	0.082
Al	0.0615	0.017
S	0.637	0.241
Pt	0.426	0.433
Total	13.7	9.8

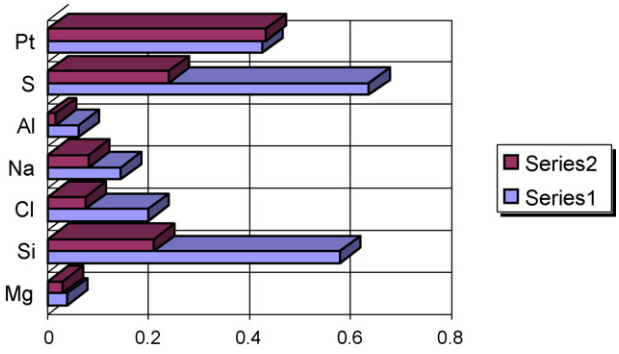

Fig. 7. XRF analysis of EMA: series 1 (anode) and series 2 (cathode).

the stoichiometry of 1.2 and 2.0, respectively. The cyclic voltammetry and ac impedance measurements were carried out with the help of Ecochemie Autolab, Model PGSTAT 30, incorporated with an ac impedance analyzer.

3. Results and discussion

3.1. Electrode characterisation

The SEM picture of the catalyst layer coated on the polyimide film is shown in Fig. 2. From the figure, one can see that there are large number of grain boundaries, cracks and voids in the catalyst layer. The SEM and EDAX spectrum, shown in Fig. 3, at two different voids in the catalyst layer of the polyimide film showed no platinum particles. However, after transferring the catalyst layer to the Nafion film, there are no cracks and voids in the film, as shown in Fig. 4. The cracks and voids disappear due to the decal process at high temperature and pressure. The EDAX spectrum also revealed the presence of platinum in the Nafion film. This can be attributed to the uniform distribution of the constituents of the catalyst layer at the Nafion film due to temperature and pressure applied during the fabrication. Fig. 5 shows the elemental map of the catalyst layer in both the decal film as well as Nafion film for carbon, fluorine, oxygen and platinum. From the figure one can see that the dispersion of platinum is more uniform in the Nafion film compared to polyimide film. In the case of other elements, there is not much difference in dispersion between substrate film and Nafion film. The interface region between the catalyst layer and the membrane was examined by SEM by cold fracturing the membrane electrode assembly at 77 K. The cut piece was oriented vertically in the SEM sample stub and the SEM pictures along with elemental map are shown in Fig. 6.

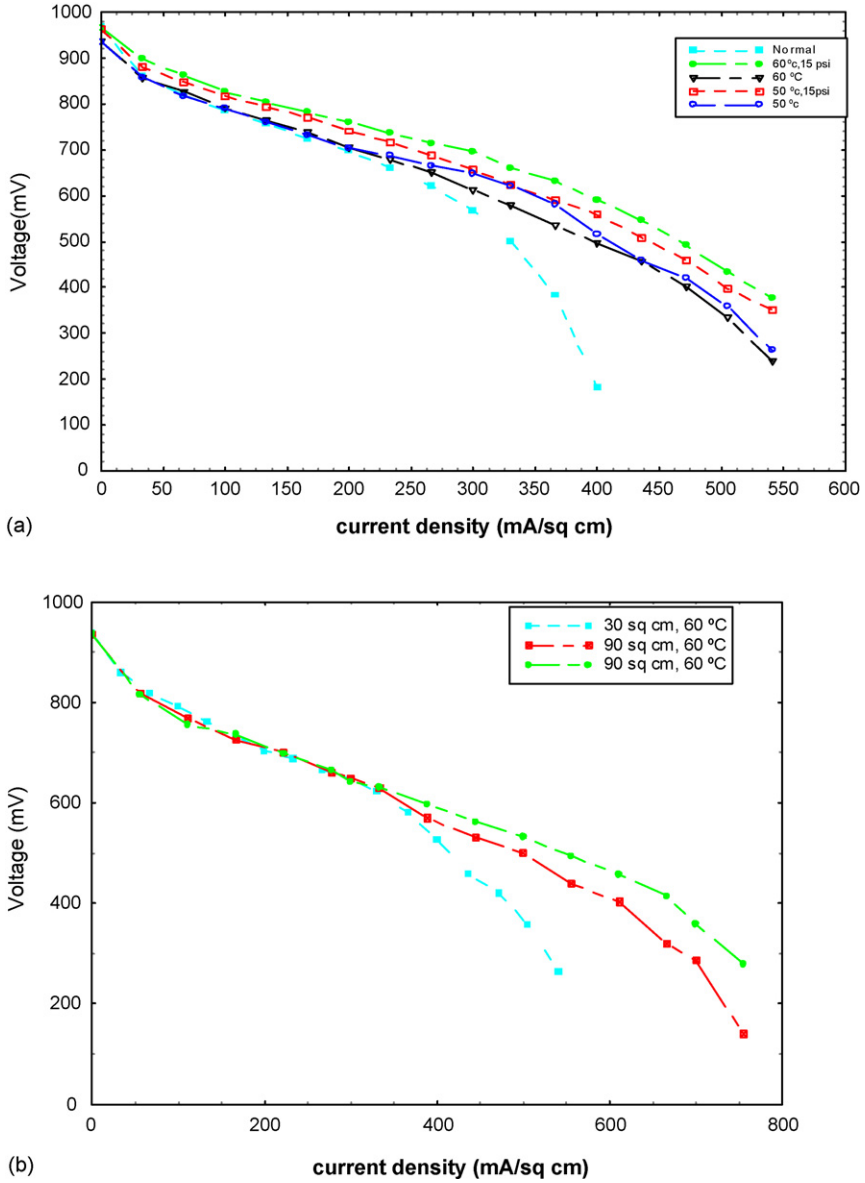

Fig. 8. (a) Current–voltage characteristics of decal electrode at various temperatures and pressures compared with normal electrode and (b) current–voltage characteristics of 90 cm^2 (two electrodes) and 30 cm^2 electrode at 60 °C.

From the elemental map one can see that the catalyst layer is on just on the surface of the film and that catalyst layer has not migrated in to the Nafion film. The EMAs were characterized by X-ray fluorescence spectroscopy (XRF) for elemental analysis and the results are shown in Table 1 which is also graphically represented in Fig. 7, after eliminating the major contribution from fluorine.

3.2. Electrochemical characterisation

The current–voltage characteristics of the fuel cell is shown in Fig. 8a. The interfacial resistance and Tafel slope were obtained from the polarization curves by fitting the polarization curve to the following equation:

$$E = a - b \log i - Ri \quad (1)$$

Table 2
Kinetic parameters of PEMFC electrodes

Electrode type	a (mV)	b (mV/decade)	R (Ω cm^2)
Normal	942.13	19.24	1.63
Decal (30 cm^2)	951.7	15.49	0.954
Decal (90 cm^2)	927.9	10.1	0.644

where E is the cell potential, a the open circuit potential, b the Tafel slope due to both the electrodes, i the current density, and R is the sum of ohmic resistance due to membrane, electrodes, contact resistance, etc. The electrodes were scaled up to 90 cm^2 by the same decal process and the current–voltage characteristics are given in Fig. 8b. The kinetic parameters are listed in Table 2. From the figure and table it is clear that the fuel cell performance for 90 cm^2 is comparable with 30 cm^2 electrode in the activation region and it performs better in the ohmic region.

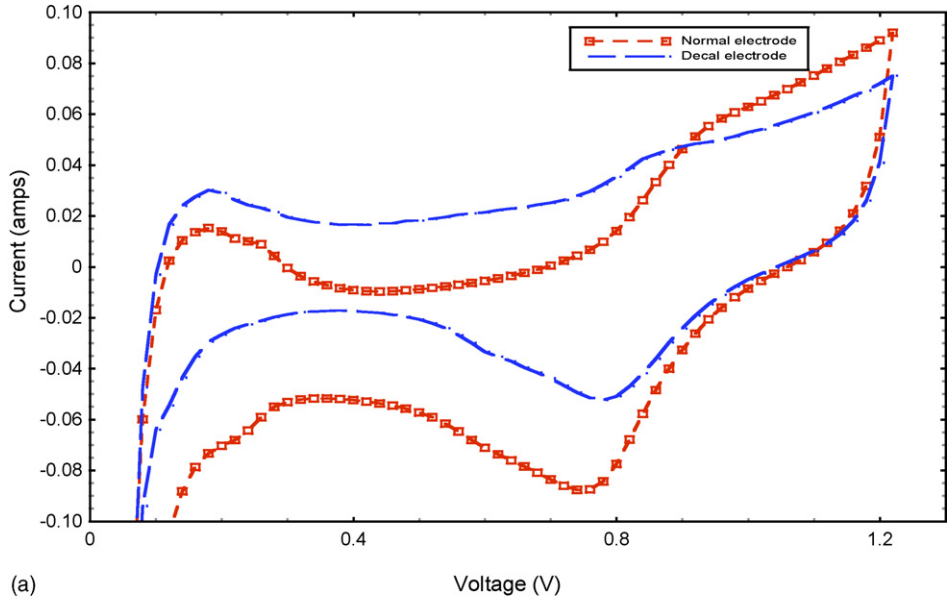

(a)

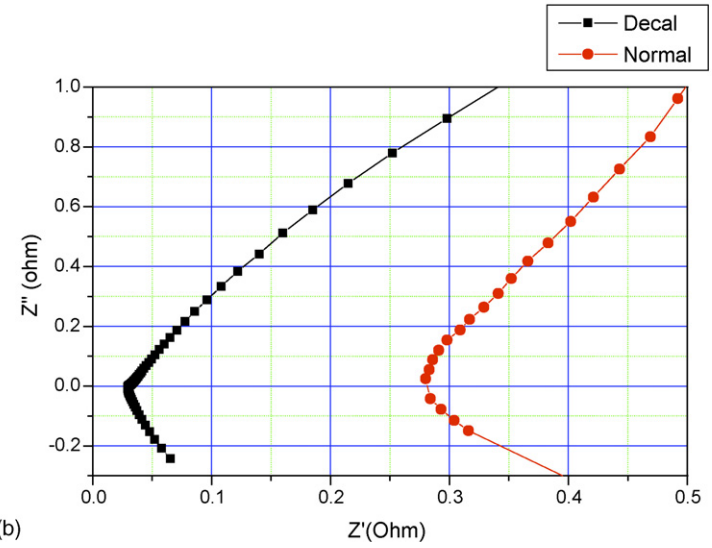

(b)

Fig. 9. (a) Cyclic voltammogram of the decal electrode and normal electrode, scan rate 15 mV/s, humidified at 50 °C and (b) ac impedance of the EMA.

From Table 2, for the normal electrode, the polarization resistance $R_p = 1.63\ \Omega\,cm^2$ reduces to $0.95\ \Omega\,cm^2$ in the decal electrode, and hence there is a decrease in overall contact resistance. This has two components viz., electronic and protonic interfacial contact resistance. The electronic contributions arising from the gas diffusion electrodes, fuel cell fixtures, compression, etc., are the same in both type of electrodes and only the catalyst layer interface with the membrane differs. Hence the drop in polarization resistance is attributed to the improved interfacial layer. This is further quantified by the following calculation for electrolyte resistance in the catalyst layer [21].

The catalyst layer electrolyte resistance can be given with respect to the tortuosity of the proton path in the catalyst layer as maximum and minimum resistance and can be computed from the following equations [21]:

$$R_{min} = \frac{1}{\sigma} - \frac{\delta}{\varepsilon_i/\Gamma} \quad (2)$$

$$R_{max} = \frac{1}{\sigma} - \frac{\delta}{\varepsilon_i^{1.5}} \quad (3)$$

where σ is the ionomer conductivity at 100 °C, 80% RH (0.13 S/cm), δ the catalyst layer thickness (0.025 mm), ε the volume fraction of ionomer in the catalyst layer (0.3 for Nafion/carbon ratio of 0.83) and Γ is the totuosity of the electrode. The Nafion to carbon ratio of 0.83 gives rise to 40% of ionomer in the catalyst layer (CL) which is optimum value required for the percolating proton network. Eq. (2) assumes the tortuosity of the path of proton travel in the CL to be equal to unity and thus gives a low-end estimate of R and when the tortuosity is considered higher end of R is obtained. The minimum and maximum resistance of the ionomer in the catalyst layer has been evaluated and is found to be 64 and 370 $m\Omega\,cm^2$, respectively.

The contributions for ohmic drop like interfacial resistance, membrane resistance and components resistance apart from ionomer, can be calculated from the polarization resistance. Since the membrane and the components and the ionomer content in the catalyst layer are the same for both normal and decal electrodes, the reduction in resistance is attributed mainly due to the reduction in interfacial resistance which is quantified by the above calculation. In the normal conventional electrode, the resistance is 1260 $m\Omega\,cm^2$, whereas for the decal electrode, it is 580 $m\Omega\,cm^2$. From this calculation it is clear that the interfacial resistance can be reduced by 50% by decal process.

The electrochemical utilization of platinum in the catalyst layer has been evaluated by cyclic voltammogram studies. The cyclic voltammogram of the electrodes with a scan rate of 15 mV/s shown in Fig. 9a, shows almost the same electrochemical platinum utilization for both the electrodes, from which it is clear that the activation region is not affected by this procedure and the improved performance is further due to reduction in ohmic contribution.

The ac impedance measurements shown in Fig. 9b, with single sine wave at 5 mV amplitude also shows the reduced polarization resistance for the decal electrode in the frequency range 100 kHz to 10 mHz. From impedance measurements, $R_p = 29\ m\Omega$, $R_{ct} = 16.56\ m\Omega$, $Z = 1.07$ F, was obtained for the decal electrodes. The double layer capacitance given by the R_{ct} is low in decal values compared to normal electrodes. The impedance was also obtained from the current interrupt method as shown in Fig. 10, where a relay switch placed in series with the load bank and the relay switch is opened while operating at a particular current and the voltage response of the cell over a given period of time is measured, which is a measure of the impedance. The fuel cell is fixed at a specific operating condition viz., load, pressure, temperature, humidity and stoichiometry. At a given time, the current relay is opened and the cell voltages are monitored for different timings viz., 0.001–0.1 s. The slope of the cell voltage response against current gives the total ohmic losses in the cell is around 64 mV, which is about 50% higher than the impedance value obtained from ac impedance, which can be attributed to the change in ohmic resistance during experiment. This can be compensated by dynamic drop compensation. Based on these experiments and calculations, the interfacial resistance between the electrodes and the electrolyte has been estimated and found to be lower by about 50% by the new process.

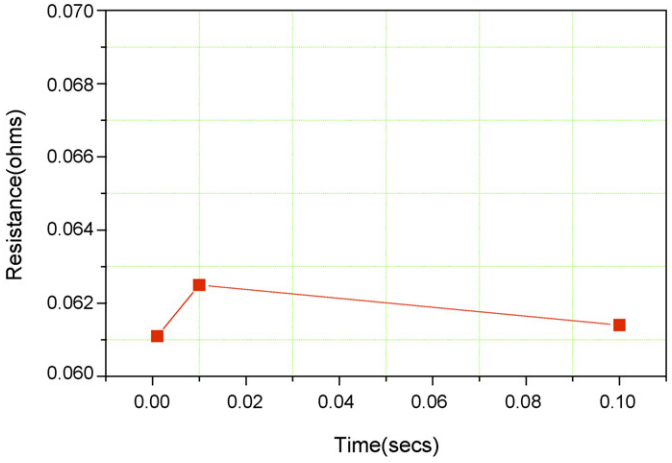

Fig. 10. Contact resistance from current interrupt method.

4. Conclusion

The electrochemical characterisation of the EMA showed a 25% higher performance increase in kinetic region current density over EMAs made by hand brushing. The ac impedance measurements also showed a lower interfacial resistance of about 50% over EMAs made by conventional method. In addition, it has been demonstrated that the screen printing and decal process is scalable. The catalyst layer by decal process also showed a higher platinum utilization in the electrodes. The current density was found to be 400 mA/cm^2 at 0.6 V for EMAs prepared by decal method compared to the current density of 300 mA/cm^2 at 0.6 V for EMAs prepared by hand brushing indicating that EMAs prepared by decal process is superior to the conventional brushing method for PEMFC application.

Acknowledgements

The authors would like to thank Dr. G. Sundararajan, Director, ARCI for his support and encouragement and Department of Science and Technology (DST), Government of India for financial assistance. We also thank Dr. K. Ravichandra (ARCI), Dr. K. Radha (ARCI) for SEM and XRF data.

References

[1] J. Maier, Nanoionics: ion transport and electrochemical storage in confined systems, progress article, Nat. Mater. 4 (2005) 805–815.
[2] M. Eickerling, A.S. Loselevich, A.A. Kornyshev, How good are the electrodes we use in PEMFC, Fuel Cell 4 (3) (2004).
[3] M. Eikerling, A.A. Kornyshev, A.M. Kuznetsov, J. Ulstrup, S. Walbran, Mechanisms of proton conductance in polymer electrolyte membranes, J. Phys. Chem. B 105 (2001) 3646–3662.
[4] T. Navessin, M. Eickerling, Q. Wang, D. Song, Z. Liu, J. Horsfall, K.V. Lovell, S. Holdcroft, Influence of membrane ion exchange capacity on the catalyst layer performance in an operating fuel cell, J. Electrochem. Soc. 152 (2005) A796–A805.
[5] M. Eickerling, A. Kornyshev, A. Kulikovsky, Can theory help to improve fuel cells, Fuel Cell Rev. (2004) 15–24.
[6] J.W. Ihm, H. Ryu, J.S. Bae, W.K. Choo, High performance of electrode with low platinum loading prepared by simplified direct screen printing process in fuel cells, J. Mater. Sci. 39 (2004) 4647–4649.
[7] R. Fernandez, P. Ferreira-Aparicio, L. Dazaa, PEMFC electrode preparation: influence of the solvent composition and evaporation rate on the catalytic layer microstructure, J. Power Sources 151 (2005) 18.
[8] Th. Frey, M. Linardi, Effects of membrane electrode assembly preparation on the polymer electrolyte membrane fuel cell performance, Electrochim. Acta 50 (2004) 99–105.
[9] R. Ben'ýtez, A.M. Chaparro, L. Dazaa, Electrochemical characterisation of Pt/C suspensions for the reduction of oxygen, J. Power Sources 151 (2005) 2–10.
[10] R. Ben'ýtez, J. Soler, L. Dazaa, Novel method for preparation of PEMFC electrodes by the electrospray technique, J. Power Sources 151 (2005) 108–113.
[11] Z. Xu, Z. Qi, A. Kaufman, Superior catalysts for proton exchange membrane fuel cells sulfonation of carbon-supported catalysts using sulfate salts, Electrochem. Solid-State Lett. 8 (2005) A313–A315.
[12] T. Kaz, N. Wagner, Investigation of the triple phase boundary of the PEFC, in: Proceedings of the 3rd European PEFC Forum, July, 2005, p. B072.
[13] D.G. Santamaria, A. Garcia-Luis, M.B. Parra, J.I. Oñate, S. Escribano, S. Solan, Reduction of Pt catalyst load in PEM fuel cells by magnetron sputtering, in: Proceedings of the 3rd European PEFC Forum, 2005, p. 419.
[14] L. Giorgi, L. Pilloni, R. Giorgi, E. Serra, M. Alvisi, G. Galtieri, A. Cemmi, C. Paoletti, M. Pasquali, Electrodeposition and sputter deposition of platinum nanoparticles on gas diffusion electrodes, in: Proceedings of the 3rd European PEFC Forum, File No. P124, 2005.
[15] J. Xie, K.L. More, T.A. Zawodzinski, W.H. Smitha, Porosimetry of MEAs made by "thin film decal" method and its effect on performance of PEFCs, J. Electrochem. Soc. 151 (2004) A1841–A1846.
[16] H. Morikawa, N. Tsuihiji, T. Mitsui, K. Kanamura, Preparation of membrane electrode assembly for fuel cell by using electrophoretic deposition process, J. Electrochem. Soc. 151 (2004) A1733–A1737.
[17] H. Kim, B.N. Popov, Development of novel method for preparation of PEMFC electrodes, Electrochem. Solid-State Lett. (2004) A71–A74.
[18] J. Wu, B. Yi, M. Hou, Z. Hou, H. Zhang, Influence of catalyst layer structure on the current distribution of PEMFCs, Electrochem. Solid-State Lett. 6 (2004) A151–A154.
[19] M.S. Saha, K. Kimoto, Y. Nishiki, T. Furuta, A fabrication method for MEAs for PEFCs using Nafion precursor, Electrochem. Solid-State Lett. 11 (2004) A429–A431.
[20] M. Inaba, H. Yamada, J. Tokunaga, A. Tasaka, Effect of agglomeration of Pt/C catalyst on hydrogen peroxide formation, Electrochem. Solid-State Lett. 12 (2004) A474–A476.
[21] R. Makharia, M.F. Mathias, D.R. Baker, Measurement of catalyst layer electrolyte resistance in PEFCs using electrochemical impedance spectroscopy, J. Electrochem. Soc. 152 (2005) A970–A977.